The Annals of Applied Statistics
2022, Vol. 16, No. 2, 627–651
https://doi.org/10.1214/21-AOAS1463

MODELLED APPROXIMATIONS TO THE IDEAL FILTER WITH APPLICATION TO GDP AND ITS COMPONENTS[1]

BY THOMAS M. TRIMBUR[a] AND TUCKER S. MCELROY[b]

Center for Statistical Research and Methodology, U.S. Census Bureau, [a]*Thomas.Trimbur@census.gov,* [b]*tucker.s.mcelroy@census.gov*

This paper examines cyclical fluctuations in a comprehensive statistical application, focusing on U.S. macroeconomic indicators related to real gross domestic product (real GDP). While GDP is generally viewed as the most widespread measure of economic activity available, our dataset also encompasses the primary GDP components, such as investment, together with leading (and regularly analyzed) subcomponent series, like residential and inventory investment. Analysis of the cycles in these major sectors provides a more informative perspective on the macroeconomic state and may improve a researcher's ability to understand and forecast cyclical movements and growth in GDP. Adaptive time series modelling is used for each time series to derive the preferred band-pass filter for computing the optimal cycle. This contrasts with the rigid use of the ideal filter, whose gain function is perfectly sharp. Regarding the ideal filter, we provide an improved implementation compared to current practice. Thus, a set of approximating filters is derived that allow for a more attractive gain profile, a better match to the targeted passband, and a direct statistical way to extract signals near the sample endpoints. Our application study demonstrates that the commonly used ideal filter can perform quite poorly on a routine basis and lead to incorrect conclusions about even the most basic questions about empirical cyclical properties. The amplitude of filtered economic activity can have major distortions and become expanded or diminished (depending on the GDP component under consideration), and many essential divergences in path may occur and affect key signals, such as expansion or contraction in growth. Statistical measures of model performance very strongly favor the adaptive parameter approach. Our statistical analysis reveals diverse dynamic behavior among the series; such results may yield worthwhile insights for output sector analysts and, even for those primarily focused on GDP, may lead to possible modelling improvements by using the finer information content in the GDP-component dynamics.

1. Introduction. The real gross domestic product (real GDP) of a nation is widely viewed as its most important indicator of overall economic activity. Such data for the United States is published each quarter by the Bureau of Economic Analysis (BEA). Each observation on real GDP measures the total value of goods and services produced over a given quarter, and data on major output components—such as investment and consumption—is also reported for the relevant time frame. The GDP-related time series may be invaluable in studying key economic issues; for instance, the study of sectors like government expenditures and exports provide baseline knowledge about issues, like the conduct of fiscal policy and the openness of the macroeconomy internationally. Also, the analysis of these data on sectoral activity also may give a more discerning picture of macroeconomic fluctuations, as described further below.

Received March 2019; revised April 2021.

[1]*Disclaimer*: This research paper is released to inform interested parties of recent work in this subject area. The views expressed on statistical, methodological, technical, or operational issues are those of the authors and not those of the U.S. Census Bureau.

Key words and phrases. Business cycles, band-pass filter, ideal filter, signal extraction, stochastic cycles, unobserved components.

In this paper we present a statistical application to both real GDP and to eleven of the most significant time series of major GDP sectors. The full dataset of 12 series in our analysis are closely related to the "business cycle" concept. This concept gives a summary of macroeconomic performance that abstracts from long-run trends and noise and focuses on medium-term or cyclical fluctuations. The business cycle incorporates the expansionary phases of the macroeconomy that are followed by recessionary periods of lower growth. There exists substantial interest in assessing how the business cycle evolves over time and on how the major economic sectors behave and relate to overall changes in real GDP as the major output aggregate, particularly in their cyclical movements. The real GDP and components data have distinct dynamic properties as regards the major expansion/recession episodes. These can have major implications for fiscal and monetary policy and for the welfare of the population; for example, unemployment can rise significantly during cyclical downturns. In our key application we concentrate on these dozen time series of central interest in economics and examine their diverse dynamics using statistical stochastic cycle models.

Stochastic cycle models have been developed in recent years to provide a dynamic summary of changing periodic-type duration around some average period, and they allow for various statistical advantages and interpretations in their application. Such phenomena occur across a vast range of scientific fields, for example, in data on sunspot activity, and the development of the necessary methodology is likely to continue for some time.

For instance, in cycles in economic data such movements typically recur with periodicity, ranging from around two to 10 years. The analysis and monitoring of such persistent and repetitive fluctuations around long-run levels are of great importance to a large population of policymakers, economists, and forecasters. The accurate estimation of such cyclical signals and their interpretation are key for understanding their role in macroeconomies and for making predictions about economic growth and business cycle transitions. In the economics and statistics literature the cyclical dynamics of the macroeconomy has received extensive attention. Examples of work concentrating on cycle estimation include Chen and Mills (2012), Rünstler and Vlekke (2018), Bulligan et al. (2019), and Gonzalez and Marinho (2017). Additional examples in economics and finance are Donadelli, Paradiso and Livieri (2019), Zizza (2006), Bashar, Bhattacharya and Wohar (2017), and Tawadros (2013).

Here, we generalize existing methodology by using a damping parameter for trend growth as a modification to Harvey and Trimbur's (2003) framework; this yields novel models and, correspondingly, more flexible filters better tailored to data properties. A problem with Harvey and Trimbur (2003) is that the filters make use of trends with ever increasing orders of integration. Here, we extend the trend so that the component remains integrated of order one, even as the persistence increases; this helps avoid implausible feature, like forecast paths given by high-degree polynomials. Thus, the generalization yields stability in trend growth. In the application below, we estimate all parameters via maximum likelihood for a dozen time series, including gross domestic product and its major components. We find clear variation in the slope damping coefficient across series and values well below unity, indicating the empirical relevance of our generalization.

In this paper we also present new explicit representations of the "ideal" filter, which has a block-shaped gain function, using a more general filter class than in Harvey and Trimbur (2003). Often an "ideal" filter with prespecified boundary frequencies has been applied to the problem of cycle measurement. The filter proposed by Baxter and King (1999) [denoted by BK filter] has been especially popular as a finite sample approximation.

Our approach improves on existing methodology for "ideal" filtering along three dimensions: the contour of the gain function, the treatment of end-point effects, and the availability of diagnostics for the filter's appropriateness. To achieve these goals, we introduce a set of representative filters that are more advantageous, compared to previous work. In particular,

we give various modelled forms of the "ideal" filter based on extensions (to account for more general trend dynamics) of the generalized Butterworth class in Harvey and Trimbur (2003). The modelled ideal (MI) filters are designed explicitly using various parameter combinations, and have a direct basis in unobserved components models that generate approximations to block-like gain functions as their optimal cycle estimators.

The MI filter solves the three key deficiencies of the BK filter. First, while the BK gain displays substantial ripples in its variation over the desired band, the MI filter's typical gain has a significantly more stable pattern and gives a far closer match to the "ideal" filter's gain function. Second, the BK filter has the drawback of truncating the extracted cycle around the end of the sample, so it omits estimates at the most important times for analysis of recent and current conditions and for making informed policy decisions; in contrast, the asymmetric MI filters that give the observation weights for near-series endpoint estimates are provided by standard algorithms or formulas. Third, the BK filter does not allow us to evaluate the viability of the ideal filter's underlying assumptions, whereas the MI filter directly makes available statistical evidence on its underlying model's performance.

The model-based band-pass filters from Harvey and Trimbur (2003) are employed in various studies of business cycle fluctuations. A leading example is the analysis in Chen and Mills (2012), who investigate estimates of the output gap in gross domestic product for the Euro area. Likewise, Busetti and Caivano (2016) study the Italian business cycle using band-pass filtering, and explore links between inflation and output in Italy. Recent work has applied structural time series models to study other important types of cycles like those in finance, housing, and credit. For instance, Rünstler and Vlekke (2018) examine cyclical components in the housing sector and their linkages with the periodic movements in economic output. More recently, Gonzalez and Marinho (2017) conduct a thorough investigation of cyclical patterns in credit and capital across 34 nations; they find that certain early indicators outperform the usual measure (credit-to-GDP ratio) in anticipating banking crises. Here, our aim is to present a generalization of the model-based filtering methodology that can be used for a very broad range of situations.

The major time series on economic activity (taken from the U.S. National Accounts) form a well-suited collection that display heterogeneous characteristics. When faced with such diverse data, there are obvious advantages to simplicity and automatic application in the use of an ideal filter; this provides a strong motivation for the current paper's examinations. However, as an offset to this benefit, there can be substantial costs to using the ideal filter. These costs depend on the input series, and may be understood by analyzing the modelled versions of the ideal filter set out below. In this fashion this paper has a primary goal of expanding available methodology and allowing for adaptive measurement of cyclical movements in statistical indicators that have various dynamic properties.

The paper proceeds as follows. Section 2 aims to clarify filter formation from underlying components, which can be used for a wide range of problems, and to show how the component dynamics in the frequency domain feed into the design of filters. The decomposition model for macroeconomic data is based on prior notions of component behavior that involve business cycle knowledge; the optimal *estimator* of the cycle then generates band-pass filter classes. This makes adaptive band-pass filtering operational through a choice of parametric models for stochastic trend, cycle, and noise components followed by optimal signal extraction. Analytical gain functions for broadly generalized Butterworth filters and the corresponding filters for related models follow from derivation of minimum mean-square error cycle estimates. In Section 3 we present the model-based representations of the ideal filter and compare them with the BK approach. With given sets of parameter values for different indices, the class of generalized Butterworth filters, along with a further generalization related to flexibility in the trend, is brought to bear on the design problem.

Section 3 further compares the modelled ideal filter to that of the BK and adaptive filters in an application to extracting economic cycles. We consider a dozen time series of national accounts data, taken from the Bureau of Economic Analysis, that include gross domestic product, investment, consumption, and other major categories of economic output. For certain series, it turns out that the cycle is either artificially dampened or incorrectly amplified by the ideal filter, whereas an adaptive filter accommodates the different cyclical intensities found among the series. Section 4 concludes.

2. Adaptive estimation of cyclical components: Explicit methodology. With the major goal of this paper being the comparison of adaptive and ideal filters, this section first highlights the basic decomposition that is implicit in the use of all filtering techniques. To provide an operational route to filter formation, we make the method practical by considering a certain class of statistical models. This entails an explicit specification of dynamics for the stochastic trend and cyclical components. This will allow us to consider examples of band-pass filters meant to target diverse gain profiles and, in particular, in the following section to design various representations of the ideal filter.

2.1. *Decomposition and unobserved components.* We first highlight specifications of time series models with stochastic trend and cyclical components. This kind of model is implicit whenever a band-pass filter is applied to extract cyclical parts in observed data subject to other kinds of movements, such as trend variation.

Band-pass filters aim to remove both low- and high-frequency movements in a time series and so can give smoother estimates and clearer indications of major transitions in the cycle. The basis for the design of a band-pass filter—its purpose and necessity—is to extract a cyclical component ψ_t, made up of a midrange frequency spectrum, from a series y_t that has other components, viz. μ_t (composed of low-frequency parts and interpretable as a stochastic trend) and ε_t which captures any remaining noise.

Explicit models are considered here that include such trend, cyclical, and noise components, whereby the observations corresponding to a sample of size T are given by

$$y_t = \mu_t + \psi_t + \varepsilon_t, \quad \varepsilon_t \sim \mathrm{WN}(0, \sigma_\varepsilon^2), t = 1, \ldots, T, \tag{1}$$

where WN denotes white noise (a serially uncorrelated process with mean zero and constant variance).

In this paper, as empirical examples, we consider applications drawn from economics for which the decomposition in (1) is quite natural and is connected with business-cycle interpretations. (Such models also hold promise for other kinds of applications in diverse fields.) Most major economic series such as real GDP have a trend dominated by frequencies at the low end of the spectrum. For an activity- or output-related variable, the trend component arises from forces such as changes in population and productivity; it is described by growth theory and evolves slowly over time. For other series, such as the unemployment rate, there may be other types of demographic factors behind the trend. The cycle component has rather different properties, representing the expansions and contractions that tend to recur around the trend as demand conditions adjust; these fluctuations have some central frequency in an intermediate (business-cycle) range. Lastly, most data in areas such as macroeconomics is subject to some sort of measurement error or is influenced by idiosyncratic effects unrelated to trend or cyclical movements, hence the need for the band-pass to cut out fluctuations at higher frequencies.

2.2. *Modelling economic fluctuations.* Here, we consider an explicit class of stochastic models of the form (1) which give a scientific and precise base for filtering methodology. This allows the use of statistical modelling principles in the problem of adaptive filter design. Our general formulation for a stochastic trend, denoted $\mu_{m,t}$, is written

$$\begin{aligned} \mu_{m,t} &= \mu_{m,t-1} + \mu_{m-1,t-1}, \\ \mu_{i,t} &= \phi\mu_{i,t-1} + \mu_{i-1,t-1}, \quad i = 2, \ldots, m-1 \end{aligned} \tag{2}$$

with $0 < \phi \leq 1$ and $\mu_{1,t}$ given by a random walk representing the core first-order process. When $\phi = 1$, this model underpins the generalized Butterworth filter in Harvey and Trimbur (2003). Here, we allow for the possibility of growth rate damping and consider $\phi < 1$ to give more flexible descriptions of fluctuations and improved model performance. Our analysis focuses attention on order $m = 2$ in (2). Such models work well empirically (particularly when the damping parameter is generalized), are relatively simple and easy to interpret, and allow us to focus on the band-pass aspect and the underpinning cyclical dynamics. Hence, we set $\mu_t = \mu_{2,t}$ in what follows.

The definition of a stochastic cycle ψ_t uses a recursion for deterministic cycles (which involves an ancillary process ψ_t^*) and augments it by adding a vector of shock variables to the right-hand side. The general process evolves as

$$\begin{bmatrix} \psi_t \\ \psi_t^* \end{bmatrix} = \rho \begin{bmatrix} \cos\lambda_c & \sin\lambda_c \\ -\sin\lambda_c & \cos\lambda_c \end{bmatrix} \begin{bmatrix} \psi_{t-1} \\ \psi_{t-1}^* \end{bmatrix} + \begin{bmatrix} s_t \\ s_t^* \end{bmatrix}, \tag{3}$$

where s_t and s_t^* are the shocks feeding into the cycle and auxiliary process, respectively. The cyclical fluctuations tend to recur with frequency λ_c, which may be interpreted as a central frequency, with corresponding period of $2\pi/\lambda_c$. The general case allows for resonance or reinforcement of the cyclicality with the model for ψ_t indexed by a positive integer n and referred to as an nth order process, denoted by $\psi_{n,t}$. The higher the order, the more the reinforcement of the periodicity around the central value λ_c and, as a result, the cycle movements increasingly focus on a frequency band surrounding λ_c.

One can also choose between "Balanced" and "Butterworth" forms of $\psi_{n,t}$. These two forms allow for slightly different roles of the stochastic part of the model; in some cases this can make a significant difference for the extracted components, as for the cycle in the residential investment series for order $n = 8$ (illustrated in Figure F.1 in Appendix F of the Supplementary Material (Trimbur and McElroy (2022))). Generally, model-fit statistics differ between the types (which may affect order choice), and filtered cycles may be different. Given these findings, it would be wise to maintain both "Balanced" and "Butterworth" models in the cycle/band-pass "tool-kit" for general applications. The two models are discussed further in Appendix E, and detailed formulations are in (E.1) and (E.5) of the Supplementary Material (Trimbur and McElroy (2022)).

2.3. *Filter design.* Now, assume that the decomposition in (1) holds with trend given by (2) and cycle following the nth order process $\psi_{n,t}$ of Butterworth form. Denote each component spectrum by $f_x(\lambda)$ for $x \in \{\psi, \mu, \varepsilon\}$. The gain of the band-pass filter that gives the optimal estimator of the cycle is

$$F_M^{bp}(\lambda) = \frac{f_\psi(\lambda)}{f_\mu(\lambda) + f_\psi(\lambda) + f_\varepsilon(\lambda)}. \tag{4}$$

This follows from the frequency domain expression of the Wiener–Kolmogorov filter that minimizes the mean-squared error of the component (see Bell (1984)). Writing this out ex-

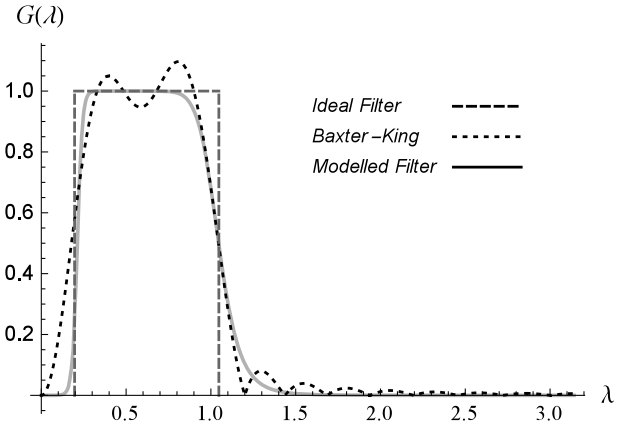

FIG. 1. *Gain functions for the model-based representation of the ideal filter are indicated by a solid gray line, for the BK filter (truncation of 12 observations at series' ends) by a dotted black line, and for the ideal filter by the dashed dark gray line.*

plicitly,

$$
\begin{aligned}
&\mathrm{GB}^{bp}_{m,n}(\lambda;\phi,\lambda_c,\rho,q_\zeta,q_\kappa)\\
&\quad= q_\kappa\left[\frac{1+\rho^2\cos^2\lambda_c-2\rho\cos\lambda_c\cos\lambda}{1+\rho^4+4\rho^2\cos^2\lambda_c-4(\rho+\rho^3)\cos\lambda_c\cos\lambda+2\rho^2\cos 2\lambda}\right]^n\\
&\qquad\Bigg/\left(q_\zeta\left[\frac{1}{(2-2\cos\lambda)(1+\phi^2-2\phi\cos\lambda)^{m-1}}\right]\right.\\
&\qquad\left.+\,q_\kappa\left[\frac{1+\rho^2\cos^2\lambda_c-2\rho\cos\lambda_c\cos\lambda}{1+\rho^4+4\rho^2\cos^2\lambda_c-4(\rho+\rho^3)\cos\lambda_c\cos\lambda+2\rho^2\cos 2\lambda}\right]^n+1\right),
\end{aligned}
\tag{5}
$$

where $q_\zeta=\sigma_\zeta^2/\sigma_\varepsilon^2$ and $q_\kappa=\sigma_\kappa^2/\sigma_\varepsilon^2$ satisfy $q_\zeta,\,q_\kappa>0$. This represents a further generalization of the Butterworth class of filters whose gain functions have relatively compact forms. The notation indicates the filter's dependence on model orders and parameter values. Expression (5) remains relatively compact, and with various choices of parameter values a diverse array of gain contours is achieved. In the next section the treatment starts directly with filtering in the frequency domain to treat representations of the ideal filter. These are based on the above model classes and provide illustrations of how one may emulate certain kinds of gain functions in band-pass filtering.

3. Ideal filter approximations: Representation and evaluation. The main goal of this section is to form model-based versions of the ideal filter to more effectively handle situations when such a filter represents a tenable approach. Note that, as a general strategy, rather than impose conditions on the gain, the current paper suggests a different approach, where the knowledge about business cycles and their periodicity refer to the components and where the filter is adapted to the input series.

Nevertheless, in certain cases an ideal filter may be a reasonable notion to entertain. Therefore, instead of going from model to filter, in this section we proceed in the opposite direction and study the model that implies a certain emulated gain function. In this case the target is the ideal filter with gain indicated in Figure 1 below. In this section the BK filter is first reviewed, and some major shortcomings are noted. The rest of the section is then devoted to the development of modelled representations of the ideal filter.

3.1. *The BK filter.* Many researchers have applied a strategy of gain emulation and have in particular sought to reproduce the "ideal" filter,[1] which has a perfectly block-like gain function, as closely as possible in a finite sample. The simple BK filter of Baxter and King (1999) represents the most popular representation for economic data. This subsection compares an approximating modelled filter with the BK version.

In macroeconomic work, Baxter and King (1999) proposed using an interval from six to 32 quarters. The targeted gain is perfectly sharp and passes through the associated periods for business cycles. The corresponding frequency range has lower limit $\lambda_l = \pi/16$ and upper limit $\lambda_u = \pi/3$. The filter has equivalent impact on the amplitudes of different frequency parts within that interval, as indicated by the dashed line in Figure 1.

Given a truncation parameter K, the BK filter may be expressed in terms of the lag operator L as

$$\mathrm{BK}(L) = \sum_{j=-K}^{K} b_j L^j,$$

where the coefficients are

$$b_j = \big[\sin(|j|\lambda_u) - \sin(|j|\lambda_l)\big]/(|j|\pi) - (c_u - c_l), \quad j \neq 0,$$
$$b_0 = (\lambda_u - \lambda_l)/\pi - (c_u - c_l),$$

with the constants c_u, c_l given by

$$c_u = \frac{\lambda_u/\pi + 2\sum_{j=1}^{K} \sin(j\lambda_u)/(j\pi)}{2K+1}, \qquad c_l = \frac{\lambda_l/\pi + 2\sum_{j=1}^{K} \sin(j\lambda_l)/(j\pi)}{2K+1}.$$

The construction of the filter involves the choice of K; increasing this parameter gives a closer finite sample approximation but leads to the omission of K estimates at both the beginning and end of the sample. The authors suggest using $K = 12$ for quarterly data as a compromise between diminished accuracy in representation of the filter and loss of information near sample endpoints.

A highly unsatisfactory aspect of the BK filter is that, in the crucial passband region of intermediate frequencies, the gain function displays large, undesirable ripples. Figure 1 shows the gain of the BK filter (the black, dotted line) vs. the "ideal" gain (dashed, dark gray line) with $K = 12$. As the frequency increases from zero, the BK gain first rises to around 1.05, then falls back to below 0.95; finally, the gain rises to nearly 1.10 before, at last, tapering off toward zero at the right edge of the passband interval. Additional oscillations in the gain function of lesser consequence occur at higher frequencies. Such ripples appear unnatural and hard to justify from the perspective of cyclical activity in economic time series. The modelled form of the ideal filter, represented by the solid gray line, weights frequencies around the midrange roughly equally and displays a gradual, continuous fall-off as the frequency moves beyond the general vicinity attributed to business cycles.

[1]The use of the word "ideal" implies an innate preference for this sharp gain function. But such a rigid prior on periods is often inappropriate for the gain, as illustrated in later sections. It may be more ideal for the filter to account for the spectral shape of the cycle consistent with the input series and with its trend; in economics we expect the cyclical part's spectral peak to lie within a vaguely defined business cycle range and which otherwise can have flexible characteristics. We use the standard terminology "ideal" in this paper only as an adjective describing the block gain shape.

3.2. *Ideal filter—modelled versions.* For the generalization of the Butterworth class of filters in (5), the five parameters $\{\phi, \lambda_c, \rho, q_\zeta, q_\kappa\}$ all have interpretations related to the implicit time series models of trends and cycles; in this section we focus on their role in determining the form of the gain function. Note that this form is more general than that in Harvey and Trimbur (2003) since it allows for values of the trend-related parameter ϕ less than unity; the merits of this added flexibility are discussed with reference to underlying statistical models below.

Given positive integers m and n, $\{\mathrm{GB}^{lp}_{m,n}(\lambda; \lambda_c, \rho, q_\zeta, q_\kappa), \mathrm{GB}^{bp}_{m,n}(\lambda; \lambda_c, \rho, q_\zeta, q_\kappa)\}$ stands for a low-pass and band-pass filter pair, each of ordered pair $\{m, n\}$ and defined mutually for internal consistency. The positive integer m denotes the low-pass index and n the band-pass index of the pair of filters; this terminology refers to the fact that n primarily influences the band-pass filter and m the low-pass filter of a given collective, though both m and n affect the precise forms of $\mathrm{GB}^{lp}_{m,n}$ and of $\mathrm{GB}^{bp}_{m,n}$ jointly. The parameter λ_c is a major frequency that determines the location around which the band-pass filter is concentrated. The parameters q_ζ and q_κ are referred to as "signal-noise" ratios for the trend and cycle, respectively, due to their connection with unobserved components models that is explained in more detail below; they influence the gains' location and spread. The parameters ϕ and ρ mainly determine the filters' width and curvature.

Expression (5) encompasses a wide variety of gain shapes for the band-pass filter which can be tuned to the desired shape by an appropriate setting of orders and parameters. The orders m, n directly affect the sharpness of the filters, with higher m being especially pertinent for more rectangular low-pass filters and higher n pertaining to sharper band-pass filters. The two filters $\{\mathrm{GB}^{lp}_{m,n}(\lambda; \lambda_c, \rho, q_\zeta, q_\kappa), \mathrm{GB}^{bp}_{m,n}(\lambda; \lambda_c, \rho, q_\zeta, q_\kappa)\}$ in a given pair work in tandem and have complementary gain functions, which tend to focus on different areas of the frequency interval, while also sharing some overlap at contiguous frequencies. Here, we are primarily interested in the band-pass member of each pair; the band-pass filter is able to extract out the midrange part of the spectrum in a way that concurs with how the low-frequency part is extracted by the complementary low-pass.

Using the parametric class given in equation (5), we can choose various combinations of parameter values to design approximating filters for the desired gain profile which in this case has the perfectly sharp profile with prespecified boundaries related to business cycle periodicity. To achieve sufficient sharpness of the gain and emulate the block-like shape of the "ideal" filter, we require relatively high values for n. For the low-pass order, we set $m = 2$; higher values could be used, but they are not necessary for generating sharp band-pass filters, and $m = 2$ is underpinned by a simple, plausible trend model (as explained below). To explore the properties of different band-pass order representations, we use three alternative values, given by $n = 4, 6$, and 8. The order n represents a choice of trade-off between filter length in the time domain (which relates to achievable accuracy of finite sample estimates) and sharpness of gain function. Other aspects of the trade-off pertain to implied statistical models; the number of total processes needed in defining the model is linked to n so that a sixth order case has 12 total cycle and auxiliary elements. Also, models with higher n require more computing time for estimation and smoothing. In theory, arbitrary positive integers could be used for m and n. However, very high values of m would imply implausible trend models, as noted later. We have experimented with filters having $m \leq 5$ without computational hurdles. In terms of the band-pass index n, values of at least 10 are feasible computationally; since the incremental differences in raising n become very slight at this point, we did not investigate even higher values, though they remain a possibility that could be helpful depending on the application.

Given the three candidate values of the order $n = \{4, 6, 8\}$, substantial sharpness in the gain also necessitates a sufficiently large damping factor; for the current application the value

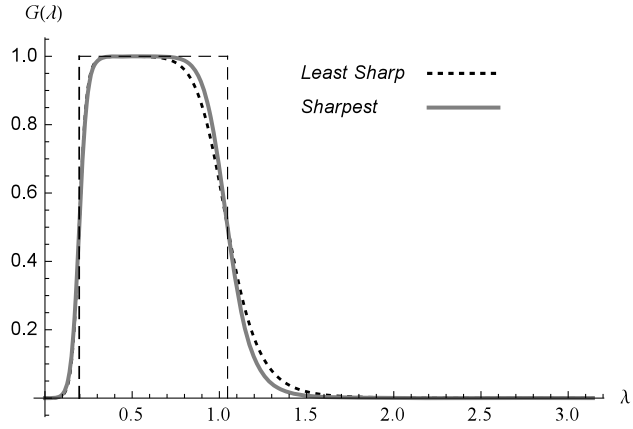

FIG. 2. *Gain functions for different ideal filter approximations with* $n = 6$, *both with* $\rho = 0.8$, $\phi = 0.97$. *For the solid and gray curve* $\{\overline{q}_\zeta, \overline{q}_\kappa, \overline{\lambda}_c\} = \{0.0124, 0.0322, 0.4910\}$, *while for the dotted and black curve* $\{\overline{q}_\zeta, \overline{q}_\kappa, \overline{\lambda}_c\} = \{2.524, 0.279, 0.398\}$. *The ideal filter is indicated by the black dashed segments*.

$\rho = 0.8$ is chosen. Lastly, a high value of ϕ (as discussed below, this relates to the persistence of trend growth) is needed, so the value 0.97 (between the lower bound of 0.95 used for quarterly data applications and unity) is used. Using the orders $\{4, 6, 8\}$ gives a broad range of gain sharpness; orders less than 4 are unlikely to produce decent approximations, while increasing the order to above 8 involves some undesirable features with excessively intense cyclical patterns in end of series estimates (this implies an extremely resonant cycle that has implausible forecasts). Furthermore, in the evolution toward a block-like filter as n rises, the benefits begin to reach a limit at very high orders; that is, the advances from 4 to 6 are more noticeable than those from order 6 to 8, whereas incremental improvements in gain sharpness become rather small after order 8.

For a given order, $\mathrm{GB}^{bp}_{m,n}(\lambda)$ also depends on the primary frequency parameter and two major q ratios, representing three remaining filter parameters: q_ζ, q_κ, and λ_c. The flexibility in the approximating gain is achieved—apart from changing n—by using different combinations $\{q_\zeta, q_\kappa, \lambda_c\}$ which are obtained as the solutions to three equations. The first two equations are composed by setting the gain equal to one-half at the business cycle boundaries, that is, $\mathrm{GB}^{bp}_{m,n}(\lambda) = 1/2$ for $\lambda = \pi/16, \pi/3$ corresponding to periods of one and a half and eight years. A third equation is formed by setting the gain equal to a high value very close to unity (the gain will never be exactly one, though it may get very close) at a midrange frequency, that is, $\mathrm{GB}^{bp}_{m,n}(\lambda) = 1 - \epsilon$, when $\lambda = 0.55$ for some small $\epsilon > 0$. This constitutes three equations in three unknowns that may be solved numerically. In practice, this was achieved using a program written in the Mathematica language of Wolfram (1996); this approach is both simple and very fast to execute. By varying ϵ monotonically and obtaining the solutions $\{\overline{q}_\zeta, \overline{q}_\kappa, \overline{\lambda}_c\}$, the designed gain is gradually adjusted in rectangular resolution and fidelity to the ideal gain.

For each n there is a certain span in the right tail's sharpness that can be attained which translates into different qualities of noise removal. To illustrate this, for $n = 6$, twelve representative combinations for a certain set of ϵ's, are selected among the various solutions; there is a single solution for each specific ϵ so that by varying ϵ different parameter triplets are obtained. As ϵ is adjusted monotonically, $\overline{q}_\zeta$ and $\overline{q}_\kappa$ also vary monotonically. Figure 2 displays the two extreme cases considered among the 12 possibilities, in the sense of being the sharpest vs. the least sharp. Ten other combinations with $\overline{q}_\zeta$ and $\overline{q}_\kappa$ lying between the values in the extreme cases are also considered. In Figure 2 the dotted black line represents the approximation with the least noise elimination, and corresponds to $\{\overline{q}_\zeta, \overline{q}_\kappa, \overline{\lambda}_c\} = \{2.524, 0.279,$

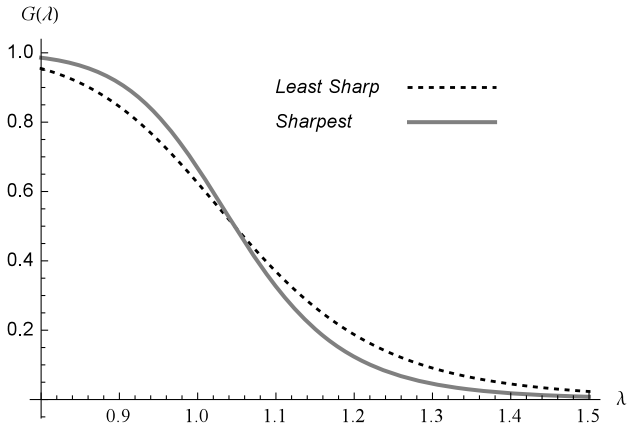

FIG. 3. *Gain functions for different ideal-filter approximations with* $n = 6$, *both with* $\rho = 0.8$ *and* $\phi = 0.97$, *shown over a specific high-frequency interval. For the solid gray curve* $\{\overline{q}_\zeta, \overline{q}_\kappa, \overline{\lambda}_c\} = \{0.0124, 0.0322, 0.4910\}$, *while for the dotted black curve* $\{\overline{q}_\zeta, \overline{q}_\kappa, \overline{\lambda}_c\} = \{2.524, 0.279, 0.398\}$.

0.398}, while the solid gray line gives the sharpest gain obtained for $\{\overline{q}_\zeta, \overline{q}_\kappa, \overline{\lambda}_c\} = \{0.0124, 0.0322, 0.4910\}$.

The close-up in Figure 3 reveals the contrast in the right-side tail in greater detail, and clearly indicates how the filter with smaller values of $\overline{q}_\zeta, \overline{q}_\kappa$ eliminates more high-frequency parts (in the figure the same line types are used for each model type as in Figure 2). The discrepancy in low-frequency removal is more modest, and is detected through examination of the close-up in Figure B.1 in Appendix B of the Supplementary Material (Trimbur and McElroy (2022)). Between these two extremes is a sequence of filters with gains enclosed by the two shown in the figures, where in each case the gain equals one-half for periods of one and a half and eight years.

A similar type of filter range occurs for the order set to 4, and the gain is less block-like than for sixth order. Figures B.2, B.3, and B.4 in Appendix B of the Supplementary Material (Trimbur and McElroy (2022)) show how, in the $n = 4$ case, the transformation of the gains, that is, the change in its descent at higher frequencies, appears somewhat larger than for the other two values of n. Thus, for $n = 8$ there is less apparent variability in the frequency response's contour among the possibilities entertained.

3.3. *Determination of ideal filter representations.* Note that the suitability of the ideal filter representation depends on the type of series in question. Hence, in Section 4 a number of major macroeconomic time series, representing GDP and its components, are analyzed to explore patterns in the appropriateness of various approximations and variation in results across data series. These 12 time series are chosen because they indicate the most important measure of activity in the domestic economy, and its major components have different dynamic properties, making it fruitful to analyze the different major components separately in order to understand overall activity. For a given series, each representation (12 combinations for each of $n = 4, 6$, and 8, so 36 in total) of the ideal filter is fitted by maximizing the log-likelihood subject to the constraints implied by the filter parameters which consist of variance ratios. The full parameter vector includes all variance parameters and slope constants that describe the series' dynamics, while the specification of $q's$ in the filter's formula omits information about a scale factor and about trend growth rates. Note that the differential behavior in the right tail of the gain function across different approximations means that different quantities of noise will be removed from an input series which will affect the

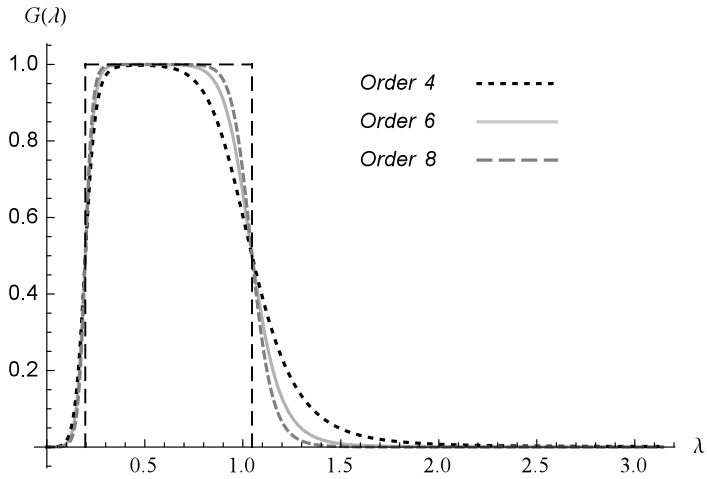

FIG. 4. *The model-based representation of the ideal filter for $n = 6$ is shown as the solid gray line. For $n = 4$, it is indicated by the dotted black line, and for $n = 8$, the ideal filter approximation is given by the dashed dark gray line.*

smoothness of the extracted cyclical signal. The estimated noise variance depends on the q values, already specified in the filter form, and relates to the observed process's scale.

For order 6, the parameter estimates are contained in table set D3 in Appendix D of the Supplementary Material (Trimbur and McElroy (2022)), while the corresponding diagnostics are reported in table set D4. For each series, various fit statistics help determine the best representation from among the 12 possibilities. Comparing these choices across the 12 national accounts variables leads to the selection of a specific representation from among the 12 candidates. For each of the three band-pass orders, a representation was selected in this way, where the aim is to focus on approximate ideal filters modelled for quarterly U.S. series related to economic activity. Details are provided below in Section 4.

Figure 4 shows the three gain functions corresponding to representations of order 4, 6, and 8. The parameter settings for $\{\overline{q}_\zeta, \overline{q}_\kappa, \overline{\lambda}_c\}$, as determined based on diagnostics and fit statistics for the collection of U.S. macroeconomic time series in our dataset, are {0.04946, 0.04589, 0.4611} for $n = 6$, {0.05722, 0.174, 0.4146} for $n = 4$, and {0.05188, 0.01226, 0.4815} for $n = 8$. In terms of fidelity to the ideal gain, there is a noticeable improvement in the approximation in going from fourth to sixth order, in that the right side of the gain around the higher frequency cutoff is more cleanly captured; components with larger frequencies are more effectively removed. Increasing the cycle index further to $n = 8$ also leads to an improved approximation, though the changes are more modest than for the transition from fourth to sixth order. There are similar alterations in the left-hand side of the gain, as illustrated in the close-up plot in Figure 5, which focuses on a subinterval of low frequencies. These differences appear small in Figure 4 but are brought out more clearly in Figure 5, once the focus rests on the more limited span of frequencies relegated primarily to trend. Similar to the high-frequency part of the spectrum, in the low-frequency area there is a significant adjustment toward a block-like gain shape as n increases from 4 to 6, and further moderate changes in moving to order 8 in Figure 5.

Figure 1 above shows the preferred ideal filter representation for order $n = 6$. Recall the most notable contrasts with the BK filter: $\mathrm{GB}^{bp}_{m,n}(\lambda)$ cuts out more low-frequency content and is far smoother than that of the BK. In applying any given filter, the effect of the operation is to take a weighted average of the observations. We compute the implied weights for the model-based version of the "ideal" filter using the "zero-one" method; these results are compared to the BK weights in Figure B.5. The patterns for the two filters appear close

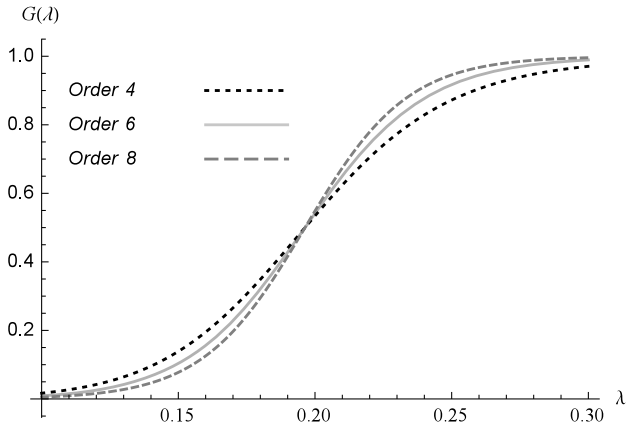

FIG. 5. *All three gain functions from Figure 4 are shown over a smaller interval of low frequencies. The model-based representation of the ideal filter for $n = 6$ is shown as the solid gray line. For $n = 4$, it is indicated by the dotted black line, and for $n = 8$, the ideal filter approximation is given by the dashed dark gray line.*

for many separations; however, there are some differences in weights that can be gleaned from the plot, in addition to nonzero weights at lags beyond the 12-period truncation for the modelled version. This divergence in the weights at bigger separations is reflected in more apparent discrepancies in the gain function, where the longer kernel of the model-based filter leads to the more attractive frequency profile, displayed in Figure B.5. Appendix B of the Supplementary Material (Trimbur and McElroy (2022)) gives some additional details on the design of suitable approximations to the "ideal" filter.

3.4. *Applications to U.S. macroeconomic series.* Quarterly data on U.S. real GDP and other national accounts indicators, such as investment, are taken from the Bureau of Economic Analysis for the period 1947 Q1 to 2019 Q3. These series are chosen because they represent the primary indicators of economic activity for the U.S.; the components of GDP behave differently from a dynamic perspective, and it is important to understand the major components to fully understand the dynamics of overall GDP. In total, 12 indicators are considered.

Starting with the unrestricted case, model (1) is estimated with the cyclical component of either the Butterworth or Balanced form for different orders n ranging up to eight. The approach is adaptive to series' individual dynamics, and all parameters are unrestricted, except for minimal constraints designed to ascertain that some type of cycle estimator, or band-pass filter, is obtained from a highly flexible and broad set of possibilities. We compute the parameter estimates for each model and series by maximum likelihood.[2] Given a feasible parameter vector, the likelihood function is evaluated from the prediction error decomposition from the Kalman filter; see Harvey (1989). The values of parameters are found by optimizing over the likelihood surface in each case. To do the calculations for the results given below, programs were written in the Ox language (Doornik (2006)).

3.5. *Parameter constraints.* The period corresponding to the central frequency, $2\pi/\lambda_c$, is constrained to lie on an interval from three and a half to eight years, ensuring that the cyclical component reflects business cycle movements rather than a different type of dynamic, such as seasonal cycles or persistent longer run patterns. Correspondingly, the periodicity conditions

[2]The difficulties associated with estimating the cyclical period for real GDP are discussed in Harvey and Trimbur (2003). For a Bayesian solution to this problem, see Harvey, Trimbur, and van Dijk (2007).

help guarantee a band-pass profile for the resulting cycle filter, meaning that the gain cuts out low frequencies sufficiently well (i.e., falls to one-half by some positive cutoff frequency as the origin is approached from the right—the midfrequency region) and likewise effectively removes the noisy part of a series' fluctuations (when the gain dips below one-half as the frequency increases from its intermediate to its maximum range).

There are two autoregressive-type parameters: ϕ for the trend slope and ρ for the cycle. The only restriction used for ϕ is to ensure its positivity; this allows the persistence in the slope to change across series. Below, it is shown how intermediate values on $[0, 1]$ are obtained that differ among series. So in the typical case, there is some regularity in growth rates of trend and a corresponding focus on low-frequency regions with the exact pattern depending on the series in questions. The interval $(0, 1)$ is used for ρ to ascertain a well-formed cycle (in practice, the actual estimates of ρ seem to always lie well within these bounds, and the occurrence of ρ very near either boundary indicates a problem with the numerical optimization).

If desired or needed, very loose constraints could be placed on the trend disturbance variance by imposing a lower bound. We experimented with numerous such cases. The lower bound ensures, at least, slightly stochastic behavior in the trend and correspondingly minimal cutting out of very low frequencies by the band-pass filters. Doing so could make the pragmatic use of the method easier. For research purposes, however, a more thorough analysis is in order to distinguish precisely between the cases of small or very small variance and of exactly zero variance. The two cases differ in their state space structure and order of integration and justify special treatments. This is related to the "pile-up problem," which was noted by a referee of the first version of the paper, where the variance estimate in maximum likelihood estimation goes to the boundary value of zero. It was found that this case was relevant for one of the series, as noted below. The specific periodicity conditions and other constraints used are detailed in Appendix A of the Supplementary Material (Trimbur and McElroy (2022)).

3.6. *Parameter estimates*. Complete results on parameter estimates, diagnostics, and fit measures are reported in Appendix D of the Supplementary Material (Trimbur and McElroy (2022)). We start by discussing the results for real GDP that are given in the first table of the set of the 12 tables of D.1. The estimates of $\widehat{\sigma}_\zeta^2$ (which denotes the maximum likelihood estimate of σ_ζ^2) show clear stochastic variation in trend growth rates. The value of $\widehat{q}_{\beta *}$, the ratio of the unconditional slope variance to total stationary variance, for the Balanced model is about 40% less than the value for the Butterworth model when $n = 1$, thus illustrating differences in how the Balanced and Butterworth model accommodate trend and cyclical movements. Also, $\widehat{\sigma}_\zeta^2$ decreases significantly in moving from first to second order. For all $n > 1$, the parameter $\widehat{\sigma}_\zeta^2$ is increasing at a modest rate and remains on the order of 10^{-5}. For real GDP, β_t can be interpreted as a growth rate of potential output. The stationary slope's mean $\overline{\beta}$ is estimated to be around 0.0077, and hence long-run potential growth is about 3.1% annually. For all orders and models, ϕ is estimated to lie between 0.55 and 0.7; intuitively, this means that the trend growth rate has moderate persistence. The slope coefficient $\widehat{\phi}$ is largest for the second order and then mostly tapers off, with smaller values seen for the Balanced process.

As n increases, for the Butterworth-type model the variance of the irregular rises consistently, with the biggest change occurring from $n = 1$ to $n = 2$. For the Balanced form, in contrast, the irregular variation reaches a peak at $n = 3$. The cyclical variation rises with n for the Butterworth-type models up to order 8, whereas it is most intense for $n = 2$ in the Balanced case. In Table D.1, the q ratio is defined precisely as $q_{\beta *} = \sigma_\beta^2/(\sigma_\psi^2 + \sigma_\varepsilon^2)$, where σ_β^2 is the unconditional slope variance and σ_ψ^2 is the unconditional variance of the cycle. The estimates of $q_{\beta *}$ fall considerably, as the model changes from first to second order cycles.

In the Butterworth model the ratio declines monotonically with increasing order. However, in the Balanced case $q_{\beta *}$'s MLE is lowest for $n = 2$ and then increases on a consistent basis with n.

The estimated value of the variance parameter σ_κ^2 declines with increasing n. For $n = 1$, the estimate of the damping parameter ρ of nearly 0.9 indicates a persistent cycle. The value of ρ also decreases for larger n. Given the resonance property of higher order cycles, where shocks are increasingly reinforced within the system, a fixed value of ρ would lead to a more pronounced cycle, as the order increases; however, there is an off-set to this effect via smaller damping parameters for larger n. For the frequency MLE for real GDP, the corresponding period is four years for all cases.

For investment, central periods within the constraining interval are estimated for most orders beyond one. In the Balanced case the period estimates rise with order and reach slightly below seven years for $n = 8$. The values of $\widehat{\rho}$ are close to those for GDP for each n. There is also a similar pattern in the decline of the cycle disturbance variance and a gain in irregular variance with rising n—in this case $\widehat{\sigma}_\varepsilon^2$ enlarges monotonically with order. Both $\widehat{\sigma}_\kappa^2$ and $\widehat{\sigma}_\varepsilon^2$ are larger in magnitude for investment, reflecting the stronger cyclical properties and greater noise content of this primary subsector of GDP. The same jump in σ_ε^2 from $n = 1$ to 2 holds for investment, with further increases tapering off as n approaches 8 (this pattern continues for even higher n than are shown in the tables). The long-run trend growth rate of investment is somewhat larger than that of GDP and likewise stable over the range of orders. The values of $q_{\zeta *}$ are considerably lower than for GDP, conveying statistically the stronger cyclical content of investment. The slope's damping coefficient is more stable and lies in the neighborhood of $\widehat{\phi} = 0.65$ for all orders.

Various aspects of the pattern of parameter estimates for real GDP and investment also hold for other series. Perhaps most notably, the irregular variance jumps in value from first to second order and then continues to steadily increase for $n > 2$, implying that ever larger amounts of noise are removed from the cycle which as a result becomes smoother as n rises. For all series, except inventory investment, the ratio $q_{\zeta *}$ is above 10^{-5} and supports the use of a stochastic model for the trend. The patterns of ρ and σ_κ^2 with respect to different n are rather similar across the different data series. Indeed, based on our overall experience with quarterly macroeconomic series, having the values of ρ and σ_κ^2 fall with n in this manner is a regular feature shared by most series related to economic cycles. The decline in these parameters at higher orders serves to mitigate some of the cycle's rise in intensity with n that is related to the resonance feature of the models.

In terms of periodicity, $\widehat{\lambda}_c$ is within the constraining interval in several cases and appears reflective of business cycles for first and higher orders; for instance, for exports, most of the central periods are between four and seven years. In other cases the period estimate lies at the upper bound of eight years. There is sizable variation across series in the estimated periods over the range of permissible orders. For the general univariate filters and methodology developed here, the use of an upper bound on the period is a valuable device to ensure the cycle remains separated from trend or other component types.

There are three points that may be noted in passing. First, the models and parameter values pertain to the historical sample; they do not pertain to a specific episode, such as the recent Great Recession which some have argued represents a different kind of cycle than the traditional business cycle, but include many years of economic fluctuations. Second, the estimates are empirical and statistical and let each individual series have its own particular kind of cycle that may be related to concepts like business, housing, and financial cycles; the estimates rely on past behavior and are free of strong assumptions, such as those incorporated in debatable economic theories. Third, a central period of eight years carries with it the possibility of actual cyclical episodes that last 12 or so years or even longer; the cycle spectrum obtained

for the MLEs of the parameters has power at lower frequencies, indicating frequency parts whose periodicity is longer than the central one. The power declines away from the cyclical midrange but still remains positive over a nontrivial range of frequencies.

3.7. *Diagnostics and fit.* Several diagnostics are reported in Table D.2. R_D^2 is the coefficient of determination with respect to first differences, and $\widehat{\sigma}$ is the equation standard error. $Q(P)$ is the Box–Ljung statistic, based on the first P residual autocorrelations. Three different values of P are used in reporting these statistics, and in each case $Q(P)$ should be compared with a χ^2 distribution with $P-4$ degrees of freedom. The Akaike Information Criterion (AIC) is defined by $\text{AIC} = -2\log\hat{L} + 2k$, where $\log\hat{L}$ is the maximized log-likelihood for each model/series combination and k is the number of model parameters. Similarly, the Schwarz Information Criterion (SIC) is computed as $\text{SIC} = -2\log\hat{L} + (\log T)k$, where T is the sample size. The AIC and SIC are comparable across different cyclical orders because the overall model is once-integrated with a stationary cyclical process for all n.

In the first table of the set in D.2 for real GDP, there is a large improvement in diagnostics and fit measures in moving from first to second order. For the Balanced form the Q(24) statistic decreases by about 65%, while the R_D^2 measure increases around 28%; the AIC drops by more than 10. The overall trough of the AIC occurs for the fourth order Butterworth and fourth and fifth order Balanced models (there is a tie to the second decimal point) which also marks the optimum order and form for R_D^2. The AIC increases by around 0.4 for the second best model, which is the fourth order Butterworth, whereas the Q(24) and R_D^2 statistics are little changed. Starting from $n = 3$, further increases in cycle index lead to a very gradual worsening of diagnostics so that, for $n = 8$, the AIC is a few units higher and the Q(24) and R_D^2 are slightly less favorable than for third order. All Q(24) and Q(32) statistics are insignificant at the 5% level for orders above one, with the smallest value occurring for $n = 4$ Balanced.

For investment the large advance in model performance for $n = 2$ from first order is also present. Further, the diagnostics continue to improve as n increases so that in the Butterworth case, the R_D^2 is over 15% higher for the eighth order compared to the second order. Likewise, Q(24) is approximately 25% lower, while the AIC decreases by about 7.0 in going from $n = 2$ to $n = 8$. The optimal performance occurs for eighth order for the R_D^2 and AIC, while order 6 performs best for the Q statistics (the diagnostics give mixed implications). There are clear merits here, in terms of model fit, in considering relatively high order specifications. In contrasting the two model forms, the Balanced cycles exhibit superior fit, compared to Butterworth type for $n = 1$ and 2, whereas for higher orders, the two forms show an increasing tendency to converge in their diagnostics. All Q-statistics lie below the 5% critical value for $n \geq 3$.

Nearly all series show improvements in fit measures in going from $n = 1$ to 2 which are often sizable. The only exception appears to be consumption of services which displays a very slight worsening in AIC and SIC along with R_D^2 and which in any event has a rather weak cycle. For seven out of 12 series, the selected order is 2 or 3; for four series the preferred index is 7 or 8. Two of the high-order selections are investment series known to have very pronounced cycles. The other two consist of consumption, which is a highly aggregated series, as well as exports, which depend on a large mix of foreign economies.

Overall, the smallest Q(24) statistics are obtained for inventory changes (in particular the eighth order Balanced model) which is almost entirely dominated by cyclical movements. Similarly, small values of Q(24) occur for real GDP, investment, and exports, with the corresponding p-values exceeding 0.1. Of these four series with favorable Q-statistics, three have intermediate central periods that are estimated within the restriction interval, being plausible for business cycle fluctuations. Overall, for all 12 series the model selection results appear

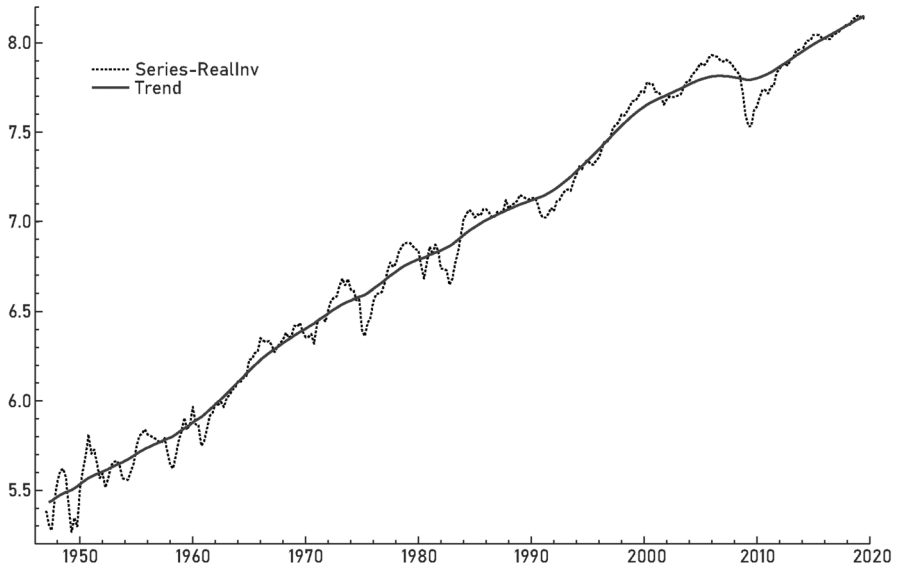

FIG. 6. *Investment (in logs) shown as the dotted black line, along with the estimated trend for $n = 6$ of Balanced form given by the solid dark gray line.*

very similar for SIC and AIC, and the implications of R_D^2 comparisons matched nearly all of the selections made based on AICs, whereas the Q-statistics sometimes lead to different conclusions.

3.8. *Smoothed components and filters.* Figure 6 shows the (logged) series of real investment along with the estimated trend (for the Balanced model with $n = 6$, corresponding to the cycle given by the solid line in Figure 8 below). The trend varies smoothly throughout the sample period, undergoing modest changes in growth rate up to the Great Recession. In the 2000s the trend decelerates somewhat rapidly and reaches a nearly flat trajectory (actually with a slight downward movement for a spell); in the recovery period after the Great Recession, the pace of growth again starts to increase so that, at the end of the sample, the slope has almost reverted to its long-run value.

Figure 7 displays the estimated cycles for $n = 1$ and 2 with the Balanced form. The use of the higher-order model is crucial to describe smoothly varying cyclical dynamics and to make transparent the primary turning points of interest to the wide audience that studies macroeconomic cycles. In contrast, the first-order model gives a noisy estimated cycle that makes it difficult to see the main transitions and general evolution. The model class with general orders can also yield sizable advances in diagnostic measures. In Figure 7 there are differences in the message given by the cycle at times, such as the 1990–1991 recession, and the Great Recession being more intense for the second-order case. The Great Recession stands out as being especially pronounced, and the overall peak-to-trough measures around five percentage points larger for the $n = 2$ case. There are likewise some strong cyclical episodes earlier in the sample period, with most of these showing a closer resemblance between first and second order, at least in terms of peak-to-trough distance. The flattening out and subsequent plunge in investment around the Great Recession is partially absorbed as a slowdown in trend growth that carries it into negative territory; this trend variability is reduced for $n = 2$ and higher.

There are further enhancements to the smooth contour of the cycle for higher orders; Figure 8 displays the extracted cyclical signals for $n = 2$ and $n = 6$. The peaks are more clearly defined for the sixth order, for instance, in the early 1960s; there are also some discrepancies in what the cycle is signaling at times, as in the 2001–02 recession which is less intense for

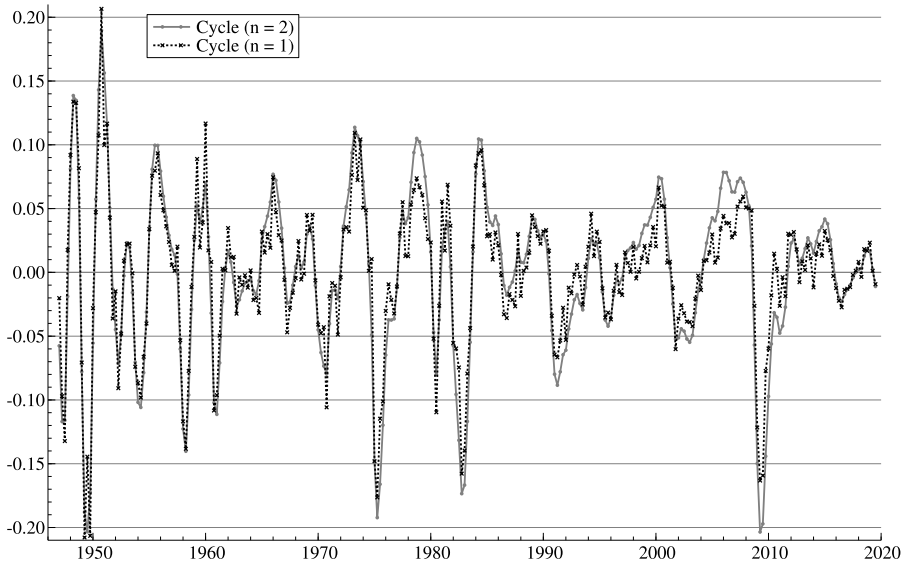

FIG. 7. *Estimated Balanced cycle in investment, shown for* $n = 1$ *as the dotted black line, and for* $n = 2$ *as the solid gray line.*

the higher-order case. The phases of increase appear more clearly demarcated, for example, the rise in the cycle into positive territory just before the decline at the end of the sample. The differences in smoothness and overall path in the two cycles along with the improvements in diagnostics make the $n = 6$ model an attractive choice (the number of parameters is the same, as just the state space dimension increases and leads to additional computing time). The extracted cycles in investment for n greater than 6 appear very similar, though there are still incremental changes, with the turning points and evolution between peaks and troughs being clearer for the higher orders. This greater smoothness is connected with how the implied filter generates a successful rendition of a band-pass that becomes sharper for higher values

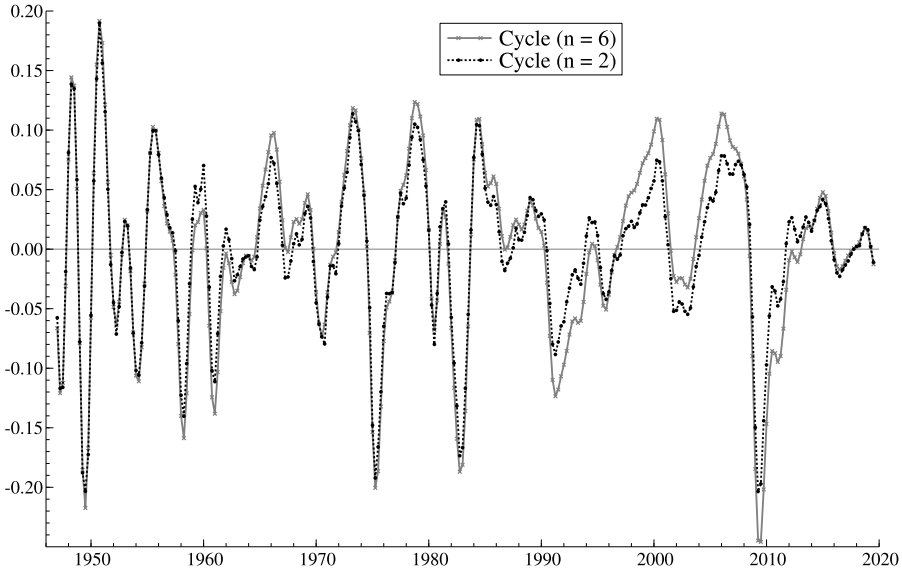

FIG. 8. *Estimated Balanced cycle in investment, shown for* $n = 2$ *as the dotted black line, and for* $n = 6$ *as the solid gray line.*

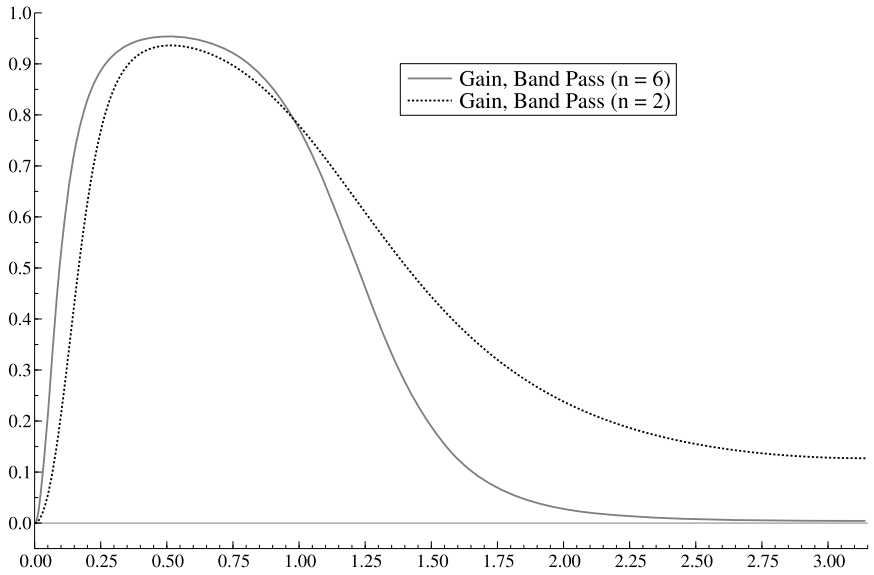

FIG. 9. *Estimated band-pass filter for extracting the Balanced cycle in investment, given by the dotted black line for* $n = 2$, *and by the solid gray solid line for* $n = 6$.

of n; the gain function is shown in Figure 9 for second and sixth orders. The higher-order band-pass effectively eliminates high-frequency movements, while the second-order band-pass admits some noise and includes it in the estimated cycle. This illustrates an advantage of high-order models, whereby the objectives of using a band-pass filter—to eliminate both trend and noise and yield smooth signals of cyclical fluctuations—are realized more fully.

For highly cyclical series there is some differentiation between the alternate forms of the cycle model. Figures F.2 and F.3 in Appendix F of the Supplementary Material (Trimbur and McElroy (2022)) show the estimated cycle and gain function for residential investment for $n = 8$ for both Balanced and Butterworth models. The Butterworth cycle displays a larger amplitude, for instance, in the 1990–91 downturn and the Great Recession, and the evolution around the sample endpoint is somewhat different. The gain function for the Balanced cycle cuts out more low-frequency movements than the Butterworth version which provides an illustration of the flexibility afforded by the different model forms.

3.9. *Comparison of parameters and filters with specific smooth trend case.* Tables D9 and D10 describe the results for the smooth trend case (the special situation where ϕ is set to unity rather than being estimated). We start by discussing real GDP. Parameter estimates are shown in the first table of the D9 set. Now, the values of $\widehat{\sigma}_\zeta^2$ are considerably smaller, as the slope shocks are permanent. The estimated variances again decrease substantially from first to second order. Thereafter, for each model type the values of $\widehat{\sigma}_\zeta^2$ increase gradually with the cycle order. The estimates of σ_ε^2 rise consistently with order for each model type; they are smaller than in the damped trend case for first and second order, but otherwise for n above two are to some extent larger in this specialized case. Likewise, the cycle variance jumps from first to second order and then declines slowly for higher n. The values are higher than for the generalized case, as the trend is less flexible, leading to more variability being accounted for by the cycle. For the smooth trend form the q ratio, now defined with numerator as the slope disturbance variance, plunges from first to second order and then increases as order rises to $n = 8$. Relative to Table D1, in Table D9 there is a similar decline in $\widehat{\sigma}_\kappa^2$ with rising n, and $\widehat{\rho}$ starts at around 0.9 and decreases monotonically with order thereafter, in the same way as

the generalized situation. The period estimate $2\pi/\widehat{\lambda}_c$ is about five years for $n = 1$, and then rises to the upper bound of 10 years for higher orders.

For investment in the second table of set D9, $\widehat{\sigma}_\zeta^2$ drops substantially from first to second order and then rises gradually to a higher value for $n = 8$. The irregular variance jumps from the lower bound to around 3 x 10^{-6} when moving from $n = 1$ to 2. For larger orders, $\widehat{\sigma}_\varepsilon^2$ grows monotonically until order 8. The value of $\widehat{\sigma}_\psi^2$ is relatively stable across model types and orders for $n > 1$. In Table D9 for investment, the estimates $\widehat{\sigma}_\kappa^2$ and $\widehat{\rho}$ decrease in similar fashion to other series and model structures. The values of $2\pi/\widehat{\lambda}_c$ are generally higher than for the generalized case as, again, the less flexible trend leads to the cycle absorbing more variability around intermediate periodicities. These patterns in parameters are shared across most of the series with some idiosyncrasies present. For instance, for investment in estimating $\widehat{\sigma}_\psi^2$ the divergence from the generalized model is lower, in percentage terms, than is the case for real GDP. For the Butterworth model for $n = 4$ to 6, the period lies around nine years. There is some diversity in values of $\widehat{\phi}$ across different time series and, within each series, across different model types and orders.

The results in the first table in set D10 reveal that, for real GDP, the Q-statistics fall significantly for all orders once the generalization is allowed. Further, the range of values in each of the three statistics, taken over all orders, are tighter for the damped-trend models. In Table D10 the minimum value for Q(24) occurs for the fourth-order Butterworth model for which there is a decline of about 20% when moving from the specific to generalized case. For the smooth trend model the AIC is minimized for the third order Butterworth case (the AIC's are not comparable across specific and generalized models, due to different orders of integration). The R_D^2 values are significantly higher in the more general case. For instance, for a fourth order Butterworth model the coefficient value increases more than 15%.

For investment all Q-statistics are enlarged when going from generalized to specialized cases. For example, for the third order Butterworth case, Q(24) increases over 40%. Table D10 reports that, for the smooth trend, the AIC attains a minimum for the eighth order Butterworth specification, as in the general structure. Likewise, R_D^2 is maximized for the same cycle model according to table sets D2 and D10. For other series the fit statistics are affected by the smooth trend restriction and may have different implications for the optimal model order and type. As an example for the time series residential investment, whose results are given in the third table of set D2 (generalized) and set D10 (smooth trend), with a smooth trend component the Butterworth third order is preferred on the basis of all three Q-statistics, and the Balanced second order is preferred, according to AIC and R_D^2. However, in Table D2 the Q(16) and Q(24) results and the AIC values imply an order 8 specification while order 7 is selected via R_D^2. Going to Table D2 from Table D10 shows consistent reductions in Q-statistics and increases in R_D^2, especially for the highest orders. For the data on nonresidential investment, there is an indication of strong preference for a second order Butterworth model for the specific case, whereas for a generalized trend the diagnostics suggest a second or third order but are more uniform across orders.

3.10. *Ideal filter approximations*: *Parameters and diagnostic measures*. Next, the selected 36 possible ideal filter approximations are applied to each of the time series considered. For each of the orders $n = 4, 6$, and 8, there are a dozen representations of the ideal filter, which are fitted to each series by maximizing the log-likelihood with respect to $\overline{\beta}$ and σ_ε^2, with filter parameters and ratios held fixed at the values determined previously. The results are given in Appendix D of the Supplementary Material (Trimbur and McElroy (2022)). Tables D3–4 pertain to $n = 6$, which is considered the benchmark representation, while D5–6 report results for $n = 4$, and D7–8 focus on $n = 8$. In each table in D3, the first two columns indicate the q ratios for each ideal filter representation; recall that q_ζ is now defined as $\sigma_\zeta^2/\sigma_\varepsilon^2$,

in line with the expression for the gain function of the generalized Butterworth filter in (5) that is linked to the model's variances. The last two columns display the MLEs; the results for real GDP are shown in the first table.

The $\widehat{\sigma}_\varepsilon^2$ values show consistent patterns of increase with falling q ratios. There is a large difference between the two boundary situations, illustrated in Figure 2, in that $\widehat{\sigma}_\varepsilon^2$ for the low q case is more than double the value for the high q case. This parallels the gain function's more effective cutting out of high frequencies with low q that is illustrated in Figure 3. Two series with a particularly large differential in noise variance are residential investment (third table, bottom of p. 2 of D3) and government expenditures (tenth table, top of p. 6 of D3), for which the maximal $\widehat{\sigma}_\varepsilon^2$ obtained is over four times the minimal $\widehat{\sigma}_\varepsilon^2$. Therefore, from the perspective of how much irregular variation is removed, it can make a significant difference how the ideal filter is represented, even after accounting for filter index. To help assess the various possibilities, we now focus on the examination of model estimation results to see which scenarios fit especially well or poorly among those considered.

Table set D2 displays diagnostic and fit statistics for adaptive results based on unrestricted MLEs. Table set D4 shows the same quantities now based on the parameter values in Table D3. For real GDP the Q-statistics are well beyond the 5% critical value, indicating decisive rejections of models that underlie ideal filter approximations. Further, the R_D^2 values are negative, indicating that the models perform worse than a random walk with drift. The results are in stark contrast to those for the adaptive models. There is a similar message for the other 11 series with varying degrees of poor fit. It would be utterly unjustifiable to entertain such models from a statistical perspective.

Sometimes, such an ideal filter might be strongly desired for any number of reasons. Therefore, it could be worthwhile to make comparisons, noting differences in how the 12 representations perform, to arrive at the best possible ideal filter models. For real GDP with $n = 6$, as shown in the first table in D4, the AIC reaches a minimum for the sixth row representation in the table that has $\{\overline{q}_\zeta, \overline{q}_\kappa, \overline{\lambda}_c\} = \{0.0661, 0.0496, 0.455\}$ which also marks the maximum R_D^2. For this representation, the Ljung–Box statistic with $P = 24$ takes on a value of about 105, compared to its minimum of just under 90 that is attained for the first row approximation; these statistics rise sharply toward the end of the table for the lowest q ratio filters. For investment with $n = 6$, the second table (D4) shows the AIC is minimum for the sixth representation, that is, $\{\overline{q}_\zeta, \overline{q}_\kappa, \overline{\lambda}_c\} = \{0.031780.040810.4709\}$. As a whole, the results indicate that AIC minimization corresponds almost always to maximization of R_D^2. Yet, minimization of $Q(P)$ frequently gives different implications. We tend to concentrate on the AIC and R_D^2, while recognizing that $Q(P)$ has important complementary information. Focusing on table set D4 ($n = 6$), the eighth row approximation ($\{\overline{q}_\zeta, \overline{q}_\kappa, \overline{\lambda}_c\} = \{0.04946, 0.04589, 0.4611\}$) appears to work best in terms of giving optimal fit and avoiding extremely poor diagnostics when all 12 series are taken as a group. Since the ideal filter tool is designed for widespread use and diverse time series, these considerations are important to bear in mind.

Tables D5 and D6 report results for the fourth order model. Table set D5 again focuses on the unrestricted parameter MLEs, while D6 contains diagnostics and fit measures. The major finding is that the results again look extremely negative, with the models explaining less of the variation than a random walk would, and with substantial serial correlation in the residuals. Doing the same exercise as before and comparing model selections across the 12 series, it appears that the seventh representation with $\{\overline{q}_\zeta, \overline{q}_\kappa, \overline{\lambda}_c\} = \{0.05722, 0.174, 0.4146\}$ works the best in terms of evading a drastically poor fit and achieving a relatively decent fit (compared to other ideal filter models). Similarly, Tables D7 and D8 report results for the eighth order for which the representation in the ninth row, which has $\{\overline{q}_\zeta, \overline{q}_\kappa, \overline{\lambda}_c\} = \{0.05188, 0.01226, 0.4815\}$, is chosen.

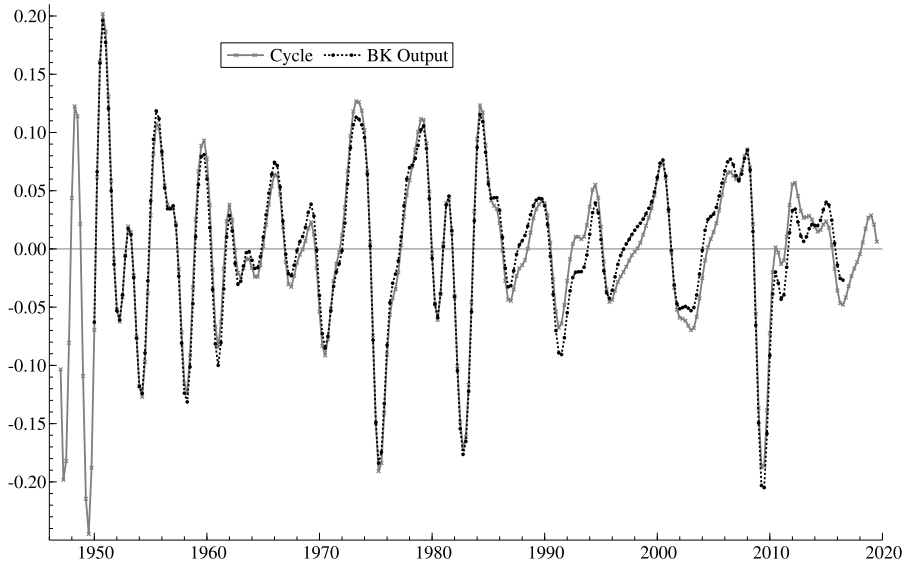

FIG. 10. *Ideal-filtered cycle in investment, shown for the BK filter as the dotted black line, and for the Balanced modelled version with $n = 6$ as the solid gray line.*

3.11. *Comparison of modelled and ideal filters.* Figure 10 displays the estimated cycle with the modelled ideal filter for $n = 6$ vs. the BK output. Over the first half of the sample, there are mostly modest differences in trajectory. In the second half there are greater discrepancies. First, the troughs in the early 1990s and in 2001–02 occur at different locations for the modelled vs. BK filter. Also, among other differences the cyclical paths in the 1990s have somewhat contrasting contours, and appear nonsynchronous. While the BK output starts to flatten out beginning in late 2001, the model-based estimates continue downward (at a more gradual rate) and reach a trough around the start of 2003 (this contrast in cyclical movements, which could be perceived as small in its relative magnitude, may, nevertheless, affect the determination of turning points). Toward the end of the series, when the BK filter truncates at a point where its output is negative and declining, the modelled cycle exhibits a bottom followed by an upswing that ends with a downward turn during the last year of the sample. These differences demonstrate how the BK gain function—with its unstable ripples and loss of information near the end-points—give a somewhat different (and more limited) path for the estimated cycle than the modelled ideal filter.

As a greater contrast, the divergence between the adaptively measured cycle and the BK output (or ideal-filtered cycle from the modelling approach) is substantial for the investment time series. Figure 11 shows the two extracted cycles. Most notably, the amplitude of fluctuations becomes significantly greater for the modelled cycle at times; this is particularly evident over the last half of the sample period. The recession of 1990–91 has a deeper trough by nearly four percentage points, whereas the peaks during 2001 and prior to the Great Recession's onset are about five percentage points higher than for the BK output. The modelled cycle starts to move down during 2008, a few quarters before the BK filtered series, which may indicate more timely turning point detection. All told, the peak-to-bottom distance is almost 15 percentage points wider over the course of the Great Recession. During the last few years of the sample, while the BK output truncates the last three years and fails to reveal the most recent developments, the estimated cycle reveals clear fluctuations reaching a trough before arriving at a modest peak, followed by some pull-back in the latest data.

Figure 12 shows the estimated gain function for investment with $n = 6$ (Balanced); ideal filter boundaries are marked by dotted lines. The gain passes through more lower frequency

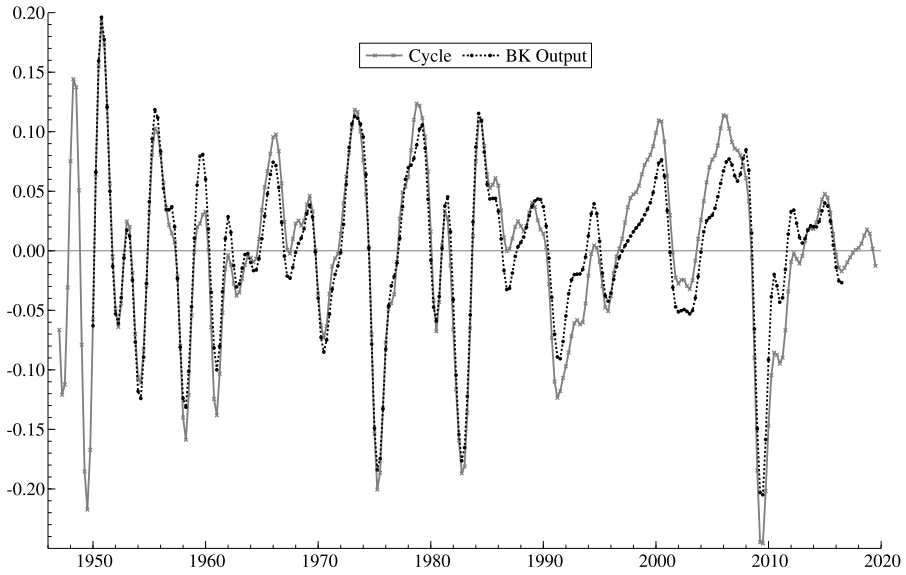

FIG. 11. *Estimated cycle* (*for the Balanced modelled version with* $n = 6$) *in investment is shown as the solid gray line. The output of the BK filter is given by the dotted black line.*

movements below the left edge. The ideal filter remains fixed and fails to adapt to the stronger cycle which makes the cross-over point (which is where the gain falls to approximately 1/2) between cycle spectrum and trend pseudo-spectrum occur at a lower frequency. The gain tapers off more gradually on the right-hand side relative to ideal filtering.

A similar comparison may be made for the major indicator of economic activity, real GDP. Figure 13 displays the extracted cycle for order $n = 4$ of Butterworth form. This particular cycle model is chosen on the basis of minimum AIC (a further digit was computed relative to the value in Table D2 in order to check for the single minimum), while other fit measures are very close to their respective minima. It can be seen that the estimated cyclical component,

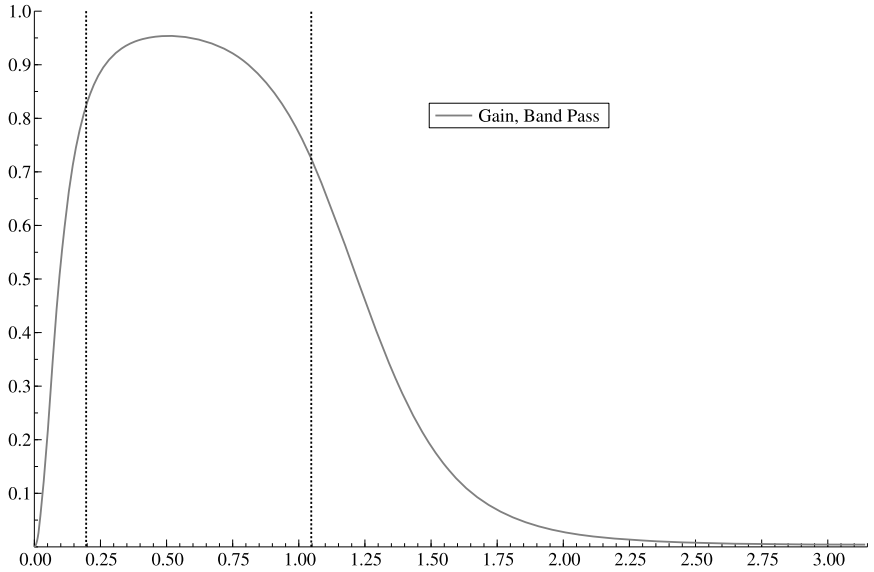

FIG. 12. *The estimated band-pass filter for extracting the cycle* (*for* $n = 6$ *with Balanced form*) *in investment is indicated by the solid gray line. Also shown are the BK ideal filter boundaries* (*dotted black lines*).

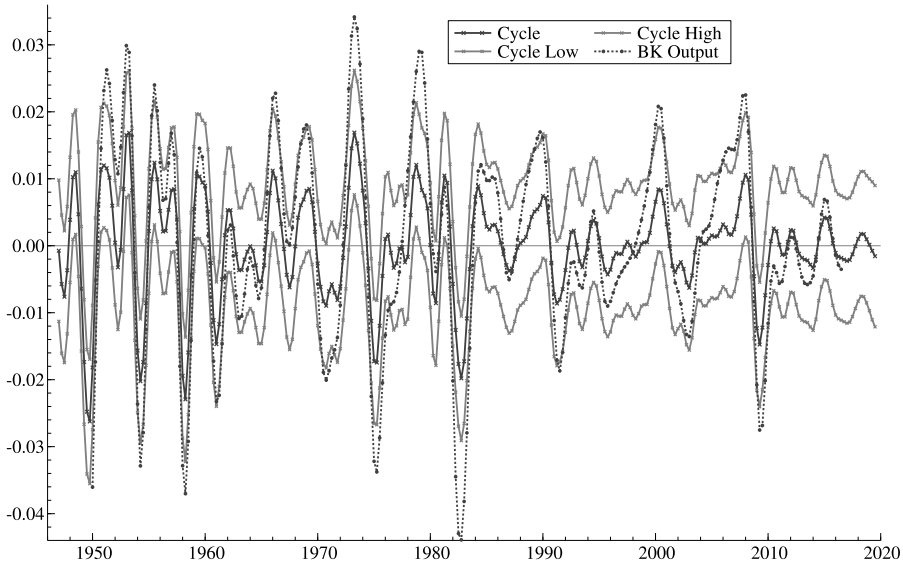

FIG. 13. *The estimated cycle in real GDP with adaptively modelled* ($n = 4$) *Butterworth form is depicted by the solid black line, with confidence bands shown as solid gray lines. The BK filter output is given by the dotted black line.*

generally, has a tighter range than the BK output. Further, confidence bands, given by one standard error above and below the actual cycle, are displayed as solid gray lines. For a significant proportion of time points, the BK output lies beyond such bands, indicating how the difference between the extracted cycle based on the series' empirical dynamics and the BK filter result has statistical significance. For many of the 12 time series analyzed here, the discrepancy between adaptive and BK cycles likewise appears significant. Appendix F of the Supplementary Material (Trimbur and McElroy (2022)) shows results for consumption of services, an additional example for which the estimated cycle is magnified by the BK filter.

4. Conclusions. This paper has examined a comprehensive dataset on U.S. real GDP and its major component time series. These series represent some of the most widely monitored data on U.S. economic activity and its breakdown into major sectors; they are of prime interest to those studying business cycle fluctuations in the macroeconomy. We have found highly heterogeneous time series dynamics, of the various sectors' output, expressed in their primary constituents of trend, cycle, and noise. Business cycle models for real GDP appears to approximately justify the use of the fixed filter known as the "ideal" filter that is emulated in Baxter and King's (1999) work. However, in several other cases among the 12 data series, the cyclical (and other) properties differ significantly to the extent that the extracted cycles and the associated band-pass filters strongly contrast with the "ideal" filter. For example, in residential investment, consumption of durables, and consumption of services, substantial discrepancies exist between the form (and general boundaries) of the property-consistent band-pass and the ideal filter emulated in previous applied work on business cycle fluctuations. In demonstrating these findings we have made further developments to the model-based filtering methodology whereby the band-pass filter for extracting the cyclical part of a time series emerges as the optimal estimator of an unobserved component cycle.

The modelled representations of the ideal filter provide a solution to the BK filter's unstable gain profile, address the sample endpoint problem associated with the BK filter's truncation, and allow one to evaluate this filter's implicit assumptions about trend-cycle relationships as well as quantifying problems of mismeasurement that may occur when indiscriminately

using such an ideal filter approximation. In certain situations an ideal filter may be used with only moderate complications, however, to know whether this is the case requires some extra effort or insight beyond the mere construction of a gain function. For strongly cyclical series, like investment, or for series such as consumption of services that have a weaker cyclical part, even basic findings about cyclical patterns can be adversely affected by use of the ideal filter approximation.

This paper instead advocates adaptive band-pass filtering *through spectral emulation, as opposed to gain emulation*, and considers methodology based on various unobserved components models. This approach recognizes that frequency domain definitions, such as those of Burns and Mitchell (1946), are intended for the cycle and are suggestive for its spectral shape. The entire premise of band-pass filtering is built on an implicit decomposition, hence the need to separate out the cycle from the observed time series by cutting out the low frequency parts linked to stochastic trend as well as the higher-frequency noise. It is intuitive that the best filter for the task capitalizes on information about how the cyclical dynamics relate to those of trend and noise. Here, we consider models that make the decomposition explicit and use a modelling framework with several advantages.

As empirical evidence we have examined 12 series drawn from U.S. national accounts data that have diverse stochastic properties and analyzed them with respect to 36 possible ideal filter representations. The basic conclusion is that the ideal filter involves a pervasive misspecification problem whose severity varies across series. Even for a series like real GDP, where the divergence of the gain function (from the optimal one) happens to be more moderate and the resulting consequences less dire, the models underpinning the ideal filter provide a poor statistical representation of the data. This is problematic for forecasting and designing policy (or making economic decisions) which routinely rely on having accurate portrayals of series' dynamics and their trend path or cyclical position. Using an adaptive band-pass provides the remedy via property-consistent extraction of cycles achieved in an econometrically optimal manner.

SUPPLEMENTARY MATERIAL

Supplement to "Modelled approximations to the ideal filter with application to GDP and its components" (DOI: 10.1214/21-AOAS1463SUPPA; .pdf). Appendices A through F.

Supplement to "Modelled approximations to the ideal filter with application to GDP and its components" (DOI: 10.1214/21-AOAS1463SUPPB; .pdf). Detailed tables of empirical results for Appendix D.

REFERENCES

BASHAR, O., BHATTACHARYA, P. and WOHAR, M. (2017). The cyclicality of fiscal policy: New evidence from unobserved components approach. *Journal of Macroeconomics* **53** 222–234.

BAXTER, M. and KING, R. G. (1999). Measuring business cycles: Approximate band-pass filters for economic time series. *Rev. Econ. Stat.* **81** 575–93.

BELL, W. (1984). Signal extraction for nonstationary time series. *Ann. Statist.* **12** 646–664. MR0740918 https://doi.org/10.1214/aos/1176346512

BULLIGAN, G., BURLON, L., DELLE MONACHE, D. and SILVESTRINI, A. (2019). Real and financial cycles: Estimates using unobserved component models for the Italian economy. *Stat. Methods Appl.* **28** 541–569. MR4009761 https://doi.org/10.1007/s10260-019-00453-1

BURNS, F. and MITCHELL, C. (1946). *Measuring Business Cycles*. National Bureau of Economic Research.

BUSETTI, F. and CAIVANO, M. (2016). The trend-cycle decomposition of output and the Phillips Curve: Bayesian estimates for Italy and the Euro Area. *Empirical Economics* **50** 1565–1587.

CHEN, X. and MILLS, T. C. (2012). Measuring the Euro area output gap using a multivariate unobserved components model containing phase shifts. *Empirical Economics* **43** 671–692.

DONADELLI, M., PARADISO, A. and LIVIERI, G. (2019). Adding cycles into the neoclassical growth model. *Econ. Model.* **78** 162–171.

DOORNIK, J. (2006). *Ox: Object-Oriented Matrix Programming Language*. Timberlake Consultants, London.

GONZALEZ, R. B. and MARINHO, L. S. G. (2017). Re-anchoring countercyclical capital buffers: Bayesian estimates and alternatives focusing on credit growth. *Int. J. Forecast.* **33** 1007–1024.

HARVEY, A. C. (1989). *Forecasting, Structural Time Series Models and the Kalman Filter*. Cambridge Univ. Press, Cambridge.

HARVEY, A. C. and TRIMBUR, T. (2003). General model-based filters for extracting cycles and trends in economic time series. *Rev. Econ. Stat.* **85** 244–55.

HARVEY, A. C., TRIMBUR, T. M. and VAN DIJK, H. K. (2007). Trends and cycles in economic time series: A Bayesian approach. *J. Econometrics* **140** 618–649. MR2408920 https://doi.org/10.1016/j.jeconom.2006.07.006

RÜNSTLER, G. and VLEKKE, M. (2018). Business, housing, and credit cycles. *J. Appl. Econometrics* **33** 212–226. MR3782759 https://doi.org/10.1002/jae.2604

TAWADROS, G. (2013). The cyclicality of the demand for crude oil: Evidence from the OECD. *Journal of Economic Studies* **40** 704–719.

TRIMBUR, T. M. and MCELROY, T. S. (2022). Supplement to "Modelled approximations to the ideal filter with application to GDP and its components." https://doi.org/10.1214/21-AOAS1463SUPPA, https://doi.org/10.1214/21-AOAS1463SUPPB

WOLFRAM, S. (1996). *The Mathematica Book*, 3rd ed. Wolfram Media, Champaign, IL. MR1404696

ZIZZA, R. (2006). A measure of output gap for Italy through structural time series models. *J. Appl. Stat.* **33** 481–495. MR2227407 https://doi.org/10.1080/02664760500448875